Supporting Information

for

A Photoionization Mass Spectroscopic Study on the Formation of Phosphanes in Low Temperature Phosphine Ices

Andrew M. Turner,[a] Matthew J. Abplanalp,[a] Agnes H. H. Chang,[b] Ralf I. Kaiser*[a]

[a]Department of Chemistry, University of Hawaii at Manoa, Honolulu, Hawaii 96822 , USA

[b]Department of Chemistry, National Dong Hwa University, Shoufeng, Hualien 974, Taiwan

*Correspondence should be addressed to Ralf I. Kaiser: ralfk@hawaii.edu

Table of Contents

Refractive index and ice thickness determination. The refractive index (n_{PH_3}) of solid phosphine and the experimental ice thickness were determined using laser interferometry. With this information, the absorption coefficients were obtained, and the details are presented below. Each laser interferogram was obtained by reflecting a HeNe laser at 632.8 nm (Melles Griot 25-LHP-213, 0.5 mW) off the silver substrate during phosphine deposition at angles shown in Figure S1. The power of the reflected light was monitored using a photodiode interfaced connected to a picoammeter (Keithley 6485), which was GPIB-interfaced to a computer and recorded using LabVIEW. The interference pattern results from constructive and destructive interference between the portion of the laser that reflects off the ice surface with the portion that transmits through the ice and reflects off the silver substrate (Figure S2). As the ice deposits, the optical path difference increases and the relative phase changes result, ideally, in a sinusoidal pattern. The refractive index was determined using a two-laser method [1] with the lasers at angles of incidence $\theta_1 = 20.0 \pm 0.1°$ and $\theta_2 = 57.0 \pm 0.1°$ and Equation 1:

$$n_{PH_3}^2 = \frac{\frac{T_2^2}{T_1^2} sin^2\theta_2 - sin^2\theta_1}{\frac{T_2^2}{T_1^2} - 1} \quad (1)$$

where T_1 and T_2 are the periods of the interference fringes for laser 1 and laser 2, respectively. A plot showing simultaneous data collection from both lasers during sample deposition is shown in Figure S3.

Our experimentally obtained value for solid phosphine is $n_{PH_3} = 1.51 \pm 0.02$. The refractive index was utilized in Equation 2 to determine the thickness (d) of the ice using the interference pattern of one laser ($\lambda = 632.8$ nm) at an angle of incidence $\theta_3 = 4°$:

$$d = \frac{m\,\lambda}{2\sqrt{n_{PH_3}^2 - sin^2\theta_3}} \quad (2)$$

Here, the fringes of the interference pattern (m) are determined using a plot such as Figure S4, which shows the interference pattern during ice deposition. Using 4.4 interference fringes, the ice was calculated to be 920 ± 20 nm thick.

Absorption coefficients. The absorption coefficients (A_{exp}) for infrared peaks were experimentally determined starting with Equation 3:

$$A_{exp} = \frac{\ln(10) \int_{\tilde{\nu}_1}^{\tilde{\nu}_2} A(\tilde{\nu}) d\tilde{\nu}}{C\, L} \quad (3)$$

where $\int_{\tilde{\nu}_1}^{\tilde{\nu}_2} A(\tilde{\nu}) d\tilde{\nu}$ is the integrated peak area (measured in cm^{-1}), C is the concentration of the ice in mol/cm^3, and L is the pathlength of the infrared beam through the ice. The concentration is related to the density of the ice (ρ = 0.90 g cm^{-3}) and the molar mass (M = 34.00 g mol^{-1}) by Equation 4:

$$C = \frac{\rho}{M} \quad (4)$$

The density determination utilized x-ray diffraction data that four molecules of phosphine (5.646 × 10^{-22} g $molecule^{-1}$) are contained in a face-centered cubic unit cell with volume 2.51 ± 0.01 × 10^{-22} cm^3.[2] The pathlength of the infrared beam through the ice, L, can be solved geometrically using Equation 5:

$$L = \frac{2d}{cos\, \theta_4} \quad (5)$$

where θ_4 is the angle at which the refracted light passes through the ice relative to the surface normal and the factor of 2 accounts for the incoming and outgoing beams. This can be related to the angle of incidence of the infrared beam (θ_5 = 43°) using Snell's Law (Equation 6):

$$\theta_4 = sin^{-1} \frac{n_v}{n_{PH_3}} sin\, \theta_5 \quad (6)$$

Noting that $cos\ sin^{-1}\frac{n_v}{n_{PH_3}} sin\,\theta_5 = \sqrt{1-\frac{sin^2\theta_5}{n_{PH_3}^2}}$ and the refractive index in a vacuum (n_v) is 1, Equations 4, 5, and 6 can be combined into Equation 7:

$$A_{exp} = \frac{\ln(10) M \int_{\tilde{\nu}_1}^{\tilde{\nu}_2} A(\tilde{\nu}) d\tilde{\nu}}{2\, d\, \rho} \frac{\sqrt{n_{PH_3}^2 - sin^2\theta_5}}{n_{PH_3}} \quad (7)$$

The experimentally determined intensities are compared with those from theoretical calculations, along with the observed and calculated peak positions, in Table S1 and reported with units cm molecules^{-1} by introducing the Avogadro constant (N_A) into Equation 7:

$$A_{exp} = \frac{\ln(10) M \int_{\tilde{\nu}_1}^{\tilde{\nu}_2} A(\tilde{\nu}) d\tilde{\nu}}{2\, N_A\, d\, \rho} \frac{\sqrt{n_{PH_3}^2 - sin^2\theta_5}}{n_{PH_3}} \quad (8)$$

Compared to results for liquid[3] and gaseous[4] phosphine, P-H stretching vibrations (ν_1 and ν_3) show similar absorption coefficients with solid phosphine. However, the values for the solid phase deformation modes (ν_2 and ν_4) were approximately a third of their liquid and gas phase counterparts. The values obtained from theoretical calculations were higher than all experimental values. Specifically, solid phosphine's experimentally determined values were 30-40% of the theoretical values for P-H stretching modes and 15-20% for deformation modes.

Because the experimental absorption coefficients for diphosphine are unknown, the theoretical value was corrected using equivalent vibrations for phosphine. Phosphine's ν_4 mode at 1096 cm^{-1} has an experimental absorption coefficient that is 19% of the theoretical value, so 19% of diphosphine's ν_{11} theoretical value was used to approximate the experimental value of 7.0×10^{-17} cm molecule^{-1}.

Table S1. Experimental and calculated infrared data for PH_3. Solid phase and calculated values were determined in this study. Absorption coefficients from liquid phosphine includes combined values for two fundamental modes.

Assignment	Experimental Frequency (cm^{-1})	Calculated Frequency (cm^{-1})	Scaling Factor	Absorption Coefficients (A_{exp}, $\times 10^{-18}$ cm molecule^{-1})			
				Solid[a]	Gas[b]	liquid[c]	Calculated[a]
v_2	982	1018	0.965	0.51	1.7	4.2	3.3
v_4	1096	1138	0.963	0.71	2.1		3.7
v_3	2303	2382	0.967	2.4	2.4	12	5.8
v_1	2308	2390	0.966	7.0	8.4		22

[a]This study
[b]Gas phase absorption coefficients[3]
[c]Liquid phase absorption coefficients[4]

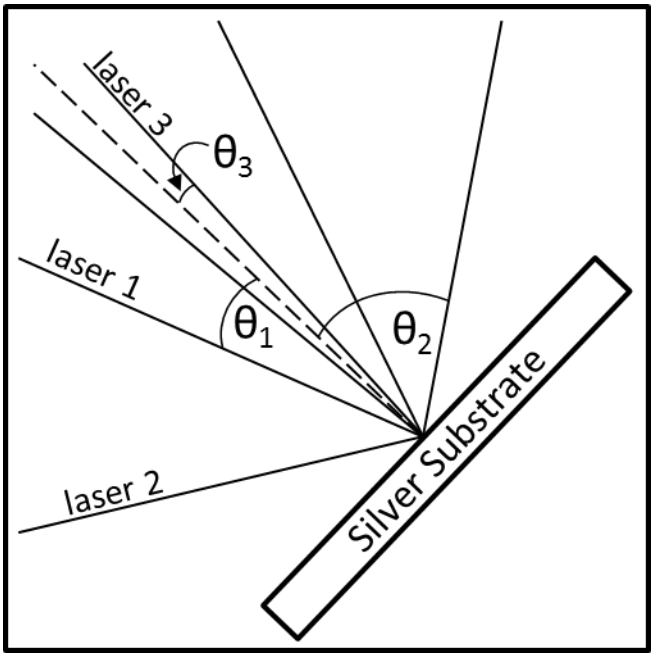

Figure S1: Diagram showing the angles of incidence relative to the surface normal (dashed line) for the three 632.8 nm lasers. The angles at θ_1 = 20.0° and θ_2 = 57.0° were used for determining the refractive index, while θ_3 = 4° was used for calculating the thickness of the ice.

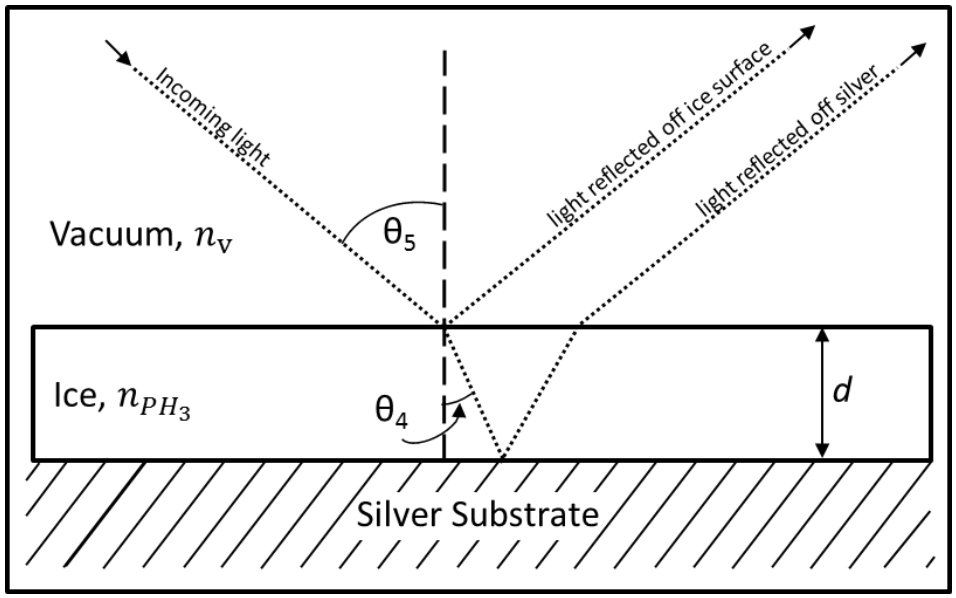

Figure S2: Diagram showing that incoming light can either reflect off the surface of the ice or pass through the ice and reflect off the silver substrate before passing out of the ice. The notation for θ_4 and θ_5 is used for the incoming infrared beam (θ_4 = 43°) in the calculation of the absorption coefficients.

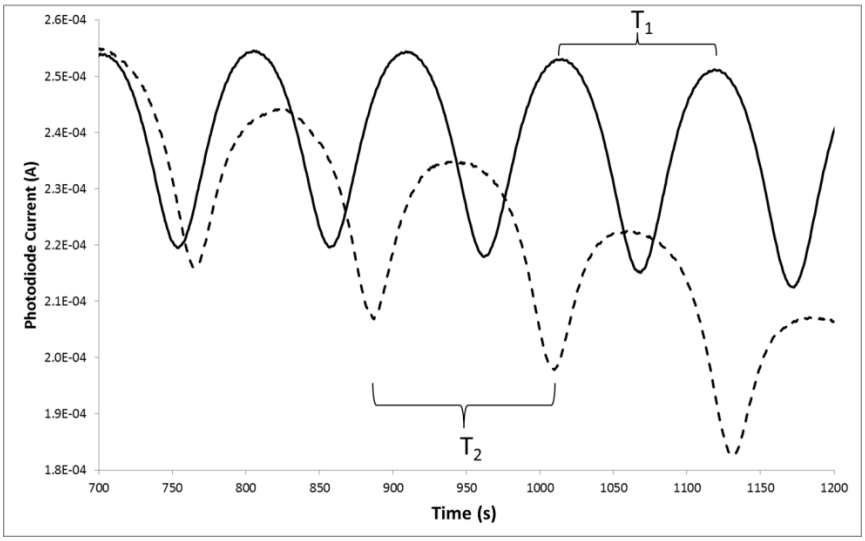

Figure S3: Interference plot for two 632.8 nm lasers striking the surface at angles of incidence of 20.0° (solid line) and 57.0° (dashed line). The distance between two extrema, measured in time, is used for values of T_1 and T_2 to calculate the refractive index of the ice.

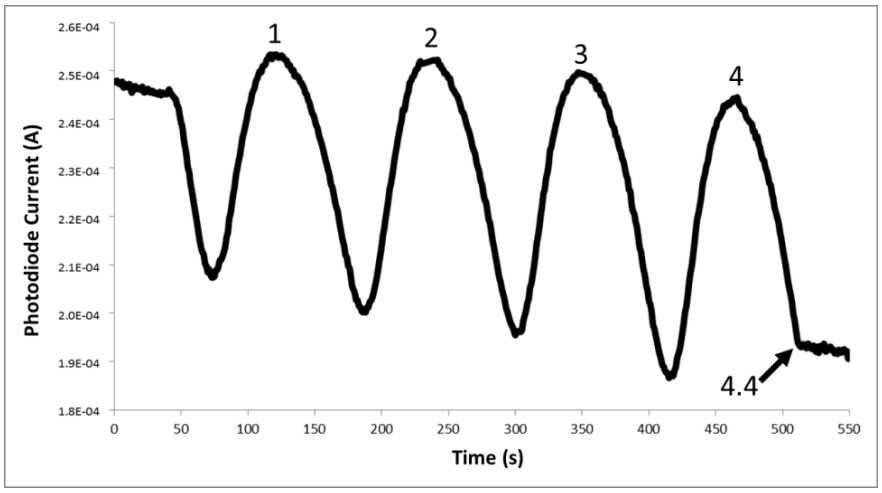

Figure S4: Interference plot for one 632.8 nm laser recorded during ice deposition at an angle of incidence of 4°. Integer numbers of fringes are labeled above signal maxima, and at the deposition stop time, 4.4 fringes had accumulated.

[1] Brunetto, R., Caniglia, G., Baratta, A., Palumbo, M. E. *ApJ*, 2008, 686, 1480.

[2] Francia, M., Nixon, E. *J Chem Phys*, 1973, 58(3), 1061.

[3] McKean, D. C., & Schartz, P.N. *J Chem Phys*, 24, 316.

[4] Sennikov, P. G., Raldugin, D. A., Nabiev, S., Revin, V., & Khodzhiev, B. *Spec Acta A*, 1996, 52, 453.